III International Conference on Particle-based Methods – Fundamentals and Applications
PARTICLES 2013
M. Bischoff, E. Oñate, D.R.J. Owen, E. Ramm & P. Wriggers (Eds)

DYNAMIC FAILURE OF MATERIALS USING THE MATERIAL POINT METHOD IN CTH

SHANE C. SCHUMACHER[1], KEVIN P. RUGGIRELLO[2] AND BRYAN KASHIWA[3]

[1]Sandia National Laboratories*
PO Box 5800 MS-0836
Albuquerque, NM 87185-0836
scschum@sandia.gov

[2] Sandia National Laboratories*
PO Box 5800 MS-0836
Albuquerque, NM 87185-0836
kruggir@sandia.gov

[3] Los Alamos National Laboratory
Post: MS B216
Los Alamos, NM 87545
bak@lanl.gov

Key words: MPM, Shock, Hydrodynamics, Failure

Summary
The dynamic failure of materials in a finite volume shock physics computational code poses many challenges. Sandia National Laboratories has added Lagrangian markers as a new capability to CTH. The failure process of a marker in CTH is driven by the nature of Lagrangian numerical methods. This process is performed in three steps and the first step is to detect failure using the material constitutive model. The constitutive model detects failure computing damage or other means from the strain rate, strain, stress, etc. Once failure has been determined the material stress and energy states are released along a path driven by the constitutive model. Once the magnitude of the stress reaches a critical value, the material is switched to another material that behaves hydrodynamically. The hydrodynamic failed material is by definition non-shear-supporting but still retains the Equation of State (EOS) portion of the constitutive model. The material switching process is conservative in mass, momentum and energy. The failed marker material is allowed to fail using the CTH method of void insertion as necessary during the computation.

*Sandia National Laboratories is a multi-program laboratory managed and operated by Sandia Corporation, a wholly owned subsidiary of Lockheed Martin Corporation, for the U.S. Department of Energy's National Nuclear Security Administration under contract DE-AC04-94AL85000.

1 INTRODUCTION

Recently marker methods have been added to a computational shock physics hydrocode named CTH. The marker methods include the Material Point Method (MPM) as a method of modeling fields as Lagrangian in CTH. The integration of the Lagrangian numerical methods expands the capabilities of CTH for solid material modeling, structural applications and fluid-structure interaction to name a few applications. The marker methods have also been integrated into the existing CTH parallel and Adaptive Mesh Refinement (AMR) frameworks allowing for massively parallel computational simulations. With the large capacity for computations, accuracy is also improved where the state of the material or structure is affected by Eulerian remap (advection) processes. Just as AMR increases the accuracy of simulations by providing refinement where needed, the inclusion of the marker methods increases accuracy through Lagrangian numerical methods.

The marker methods are built upon Lagrangian numerical concepts, therefore the marker fields do not use the Eulerian advection processes. Previously, CTH was a pure Eulerian computational shock physics hydrocode. This entails a numerical cycle that includes a Lagrangian step with a remap step (advection) that forms the Eulerian numerical method. When using the marker methods, the remap step for a marker field is not necessary and therefore not performed for the marker field within a CTH computational cycle. Another benefit of the marker method is that it utilizes the existing constitutive models within CTH. The material model physics are the same whether used in CTH or with markers.

Specifically, the MPM method provides another mechanism for modeling fracture mechanics within CTH. Previously the only method of fracturing fields was through void insertion. With the MPM method damage, fracture, etc. are stored on the marker itself. Therefore, quantities of damage or other field state variables may dictate the individual marker failure. Once the marker fails, the marker may be switched to another marker or CTH material that is hydrodynamic or non-shear supporting. This non-shear supporting material may fracture once again using CTH void insertion. This will occur if the failed material experiences a tensile state further in the analysis.

2 METHODOLOGY

The marker methods are in essence a particle method, but defined here as a marker, where a marker “marks” the material or field presence in the computational cell. The marker presence is defined as the state of the marker based on mass, location, velocity, extra (state) variables, etc.. The markers do not communicate between each other and instead use a background grid to track and communicate between each other, whether Eulerian (CTH fields) or other marker fields. The collection of markers moves according to the center of mass of the field. The state of the field is interpolated between the marker field and the background grid for interaction with other fields.

The marker numerics are broken into two processes that are coupled, the hydrodynamic state and the strength state of the field. The fluid behavior entails the field variables, pressure

P, temperature T, energy E, specific volume ν and the state or extra hydrodynamic variables denoted as *eos. The hydrodynamic state of the field is computed on the CTH background grid. The strength behavior entails the stress σ or the deviatoric stress state σ' and the state or extra variables *. The strength of the marker field is computed using the Material Point Method. The marker methods utilize the strength of two numerical techniques, Eulerian for the hydrodynamic behavior and Lagrangian for the strength and failure of the field. An important note is that the hydrodynamic state of the field is updated to the marker field after the Equation of State (EOS) computation at the bottom of each cycle, denoted as n (where n is the current cycle number). This is a complete rewrite or reset of the marker field based on the background EOS grid data. In CTH, the EOS computation is performed at the bottom of the cycle (n) to compute the new pressure for the (n+1) cycle. Fracture in CTH is performed at the bottom of cycle (n) after the EOS update.

The Material Point Method (MPM) is based on Fluid-Implicit-Particle (FLIP) [1] but with the addition of strength mechanics on the markers [4]. The implementation of MPM in CTH is performed by interpolating data between the marker field and the CTH grid. The CTH grid is used to communicate between fields either MPM or CTH. MPM computes accelerations from the marker field and the results are communicated to the grid vertices. The mixing of the field accelerations is performed at the grid vertices, where all materials in the computation are mixed conserving momentum. By definition, CTH uses a single velocity field with non-equilibrium field pressures, temperatures, energies and densities. Therefore, all materials have the same velocity at a vertex and/or cell face. A detailed summary of the marker numerical implementation process in CTH is found under Schumacher et. al. [3].

The failure of a field consisting of markers is different than that of CTH. In CTH without marker fields, the failure is dictated by the cell stress and pressure. In a mixed cell, void will be inserted based on the mixed cell properties of stress and pressure. When critical values of stress or pressure are reached, the density of the material is increased and through the EOS the field pressure is reduced. The increase in density produces a "gap" or void where the previous state of the material existed. In the case of models computing damage, etc. a scaled stress or pressure must be used to control the insertion of void. An example is shown in the following equation,

$$P^{fracture} = (1 - D) * P^{0} \, . \qquad (1)$$

where $P^{fracture}$ is the fracture criteria, D is the degree of damage in the material and P^0 is a defined initial value. The degree of damage is defined by a model typically bound from $0 \geq D \leq 1$. In contrast, markers are allowed to fail based upon the user defined field failure criteria and failure detection is performed on a marker-by-marker basis. The failure of a marker may be controlled by the damage, fracture, etc. state of the marker. For example in Eq. 1 above, the marker may fail by D = 1, rather than the functional form of Eq 1. As an option, the failure may be controlled by the functional form as in Eq. 1 on a marker.

Once a marker has failed, the marker is moved to another field. The new field is either another marker field or a CTH field. In both cases, the field is purely hydrodynamic (does not

support shear stresses). In addition, after the detection of failure on a marker, the marker stress is reduced in an inverse exponential fashion by the following equation,

$$\bar{\bar{\sigma}}_s^{n+1} = 0.6\bar{\bar{\sigma}}_s^n \ . \tag{2}$$

The 0.6 factor was investigated and little historic relevance could be found. The best explanation is that the 0.6 scaling factor is an approximate tangent slope of an exponential decay curve. Based on trial and error of other values, the most stable value was found to be 0.6 using a test suite of problems. The scaling factor is also used when reducing the accumulation of total deviatoric stress power during fracture when attempting to conserve total energy. The recoverable or elastic deviatoric stress power is reduced and subtracted from the total deviatoric stress power by the following equation,

$$e^{n+1}{}_{s\_stressp\_new} = e^{n}{}_{s\_stressp} - e^{n}{}_{s\_stressr}(1-0.6)^2 \tag{3}$$

where $e_{s_{stressr}}$ is the accumulated recoverable energy due to the deviatoric stress. Another energy option has also been added, where the irrecoverable stress power is only computed. This method does not adjust the energy by the 0.6 factor since the change in internal energy is all due to damage, plasticity, etc. processes. Current research is in progress to release stresses and energies in the fields based on physics where crack initiation, propagation, energy release, etc. are all being simulated.

Once the marker stress is reduced to a given factor, currently set at 1e6 dynes/cm^2 (~ 1 atm) the field is switched to a hydrodynamic field representing the failed field. This process moves the state of one marker to another marker or CTH field that is purely hydrodynamic in nature. The state of the marker to be move is described as M_s, P_s, e_s, ν_s, $\bar{u}_s$ and field EOS state variables. The last point to be noted is that the failed field may also fail, where void is inserted using the current CTH methodology. The void insertion method only works when the field is in tension (tensile pressure). Using the EOS portion of the constitutive model, the pressure in the field is reduced by increasing the density as described above.

3 EXAMPLE

An example demonstrating the failure methodology is the penetration of a 6061-T6511 aluminum block by a 4340 sound nose steel penetrator [2]. The aluminum target is a cylinder, 25 cm diameter x 30 cm length. The penetrator is 4340 vacuum-arc remelted (VAR) spherical nose cylindrical penetrator, body of 7.11 mm diameter x 71.1 mm length. The spherical nose is 7.11 diameter making the total penetrator length of 74.655 mm length from tip to tail. Tests were performed at several velocities with depth of penetration, pitch and yaw all recorded for each experiment. The experiment chosen below is at 841 m/s with 0 pitch and 0 yaw. The depth of penetration from the experiment was measured at 91 mm into the target. The simulation was setup axis symmetric where the pitch and yaw are 0 respectively. The simulation mesh size is 1 mm x 1 mm, with 4,592 markers in the penetrator and 600,000 markers in the target. Typical runtime for the solution is approximately 30 minutes in serial.

Convergence of the solution was determined by altering the grid size and marker counts per cell where the solution presented below is adequately converged.

The results are shown below, in Figure 1 the initial example problem setup is shown. Figure 2 shows the final penetration depth of the penetrator into the target. The unfailed materials are blue for the steel and gray for the aluminum target. The failed material is red for the steel and brown for the aluminum. From the simulation, ejecta are seen leaving the target, primarily aluminum material. The current penetrator to target interaction is fully coupled or "welded" based on the single velocity field within CTH. Therefore, possible premature failure/oblation of the penetrator is seen at the interface. The depth of penetration from the experiment was measure at 91 mm. The simulation results agree well with the experimental results at 92 mm.

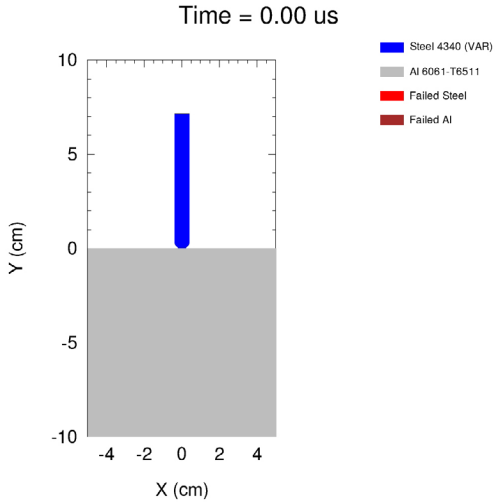

Figure 1. Example Problem Setup, 6061-T6511 Target and 4340 VAC penetrator.

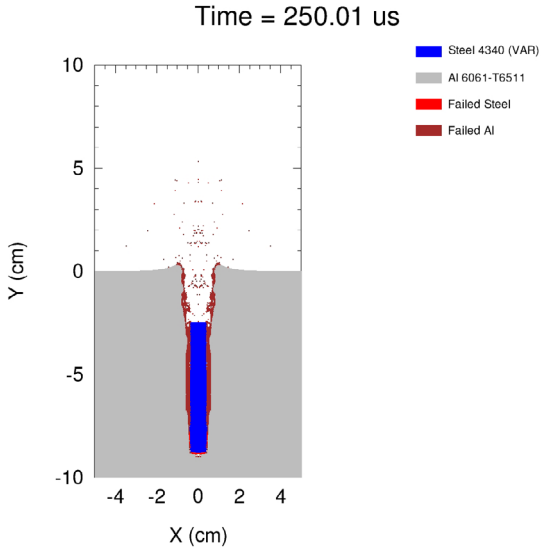

Figure 2. Penetration of 6061-T6511 Target by a 4340 VAC penetrator @ 250 μs.

4 CONCLUSION

The failure methodology for marker fields using the Material Point Method (MPM) has been presented above. This methodology is applicable to all the failure models in CTH where there is large reduction of strength when the field is highly damaged or failed. The process is a three-step process of detection, reduction and switching. The strength/failure model controls the detection of failure where several failure models exist in CTH to detect the failure of a marker. The reduction of the stress field is currently a scaling factor applied to the stress field, but physical models may be implemented to reduce stress, energy, etc. in simulation of particular failure phenomena. There are models that predict failure but retain a residual strength. These models typically predict a bulking behavior, etc. in the failed material. In these cases, the material switching is not performed as the failed material would not be strength supporting.

The example presented above provides a demonstration of the failure methodology. The material switching method is shown where the failed materials are indicated by the color change in the simulation. The simulation shows good agreement to the experimental results, as the depth of penetration is the metric of measurement.

REFERENCES

[1] Brackbill, J.U. and Ruppel, H.M., FLIP: A Method for Adaptively Zoned, Particle-In-Cell Calculations of Fluids in Two Dimensions, Journal of Computational Physics, 65, 314-343 (1986)

[2] Forrestall, M. J. and Piekutowski, A. J., Penetration Experiments with 6061-T6511 Aluminum Targets and Spherical-Nose Steel Projectiles at Striking Velocities Between 0.5 and 3.0 km/s, International Journal of Impact Engineering, 2000, 24, 57-67

[3] Schumacher, S.C., Ruggirello, K.P. and Kashiwa, B., CTH Marker Lagrangian Capabilities, 83rd Shock and Vibration Exchange, New Orleans, LA, November 4-8, 2012

[4] Sulsky, Deborah, Chen Z. and Schreyer, Howard L., A Particle Method for History-Dependent Materials, Computational Methods Applied Mechanical Engineering, 118, 179-196, (1994)